Astron. Astrophys. 354, 749–759 (2000)

ASTRONOMY AND ASTROPHYSICS

# Shear-driven wave oscillations in astrophysical flux tubes

**A.D. Rogava**[1,2⋆], **S. Poedts**[1⋆⋆], **and S.M. Mahajan**[2,3]

[1] Centre for Plasma Astrophysics, K.U.Leuven, Celestijnenlaan 200B, 3001 Heverlee, Belgium
[2] Abdus Salam International Centre for Theoretical Physics, 34014 Trieste, Italy
[3] Institute for Fusion Studies, The University of Texas at Austin, TX 78712, USA

Received 7 June 1999 / Accepted 19 November 1999

**Abstract.** In plane-parallel flows velocity shear couples magnetohydrodynamic (MHD) wave modes and induces their mutual transformations. Since the majority of astrophysical flows are not plane-parallel it is important to clarify whether this non-modal phenomenon also takes place in flows with a more complicated spatial geometry and kinematics. The recently devised local method for studying *linear* perturbation dynamics in flows with arbitrary kinematic complexity is tailor-made for this actual problem. In this paper we apply this new method to the study of velocity shear induced wave transformations in a *cylindrical flux tube*. We found that the MHD modes sustained by the flux tube flow—the Alfvén (AW), the slow magnetosonic (SMW), and the fast magnetosonic (FMW) waves — are efficiently coupled through the agency of the velocity shear. Based on this issue we argue that the individual wave transformation events, happenning perpetually and irregularly in the whole space occupied by the flux tube flow, establish the regime of *shear induced wave oscillations* throughout the flow. We claim that this previously overlooked linear phenomenon may be important for the generation of solar hydromagnetic waves, for the transmission of the waves through the transition region, for coronal heating and for the acceleration of the solar wind.

**Key words:** magnetohydrodynamics (MHD) – plasmas – waves – methods: analytical – methods: numerical

## 1. Introduction

A large majority of astronomical objects could be aptly christened as *astrophysical plasma flows*. Since the dynamical causes of plasma motion (e.g., gravitational and electromagnetic fields, pressure/temperature gradients, etc.) are spatially inhomogeneous, the resulting flows also tend to be spatially inhomogeneous on astronomical length scales. A typical astrophysical plasma flow, therefore, can be safely presumed to be a *shear flow*.

There is clearly a tremendous diversity in the general nature, geometry and kinematics of the astrophysical shear flows which range, for instance, from the cometary tails, planetary atmospheres, and stellar winds to accretion columns, accretion disks, self-gravitating galactic gaseous disks and jets. These flows provide affluent grounds for revelation of the velocity shear induced physical effects.

Since the majority of astrophysical flows is magnetized, it is of principal importance to clarify how velocity shear influences MHD collective phenomena (waves and instabilities) occurring in these flows. Evidently, the *homogeneous* steady flow may only evoke a Doppler shift in the wave frequencies, while when the flow is *inhomogeneous*, it may influence the wave dynamics in a more crucial way. Everything depends on the ratio of the flow velocity to other characteristic speeds and on the degree of spatial imhomogeneity (largeness of existing velocity gradients). Slower plasma flows in the solar corona, for instance, may act as MHD waveguides (Nakariakov & Roberts 1995) and slightly modify the dispersive characteristics of magnetoacoustic waves (Nakariakov, et al. 1996), but do not lead to any drastic changes in wave propagation. Smoothly inhomogeneous steady flow may lead to the phase mixing of the Alfvén waves, increasing their dissipation rate and creating a possibility for the *nonlinear* generation of obliquely propagating fast magnetosonic waves with a frequency and wavenumber that is twice that of the Alfvén wave (Ryutova & Habbal 1995; Nakariakov et al. 1998). When the mean flow speed exceeds the phase speed of one of the modes, the mode may become over-stable due to the negative energy wave instabilities (Ryutova 1988; Joarder et al. 1997). In more energetic (faster) flows super-Alfvénic transversal shifts/gradients in the flow velocity may incite the Kelvin-Helmholtz instability (KHI) (Parker 1964; Ferrari et al. 1981; Singh & Talwar 1994). The same kind of velocity shift may provoke the spontaneous generation of fast magnetosonic waves along the shifted layer due to the effect of over-reflection (McKenzie 1970; Nakariakov & Stepanyantz 1994).

All these linear and nonlinear effects, associated with the presence of nonzero velocity shear in astrophysical plasma flows are considered within the framework of the normal mode approach. However, by means of non-asymptotic analytical tech-

*Send offprint requests to*: Andria D. Rogava

⋆ On leave from Abastumani Astrophysical Observatory, Kazbegi avenue 2a, 380060 Tbilisi; and Department of Physics, Tbilisi State University, Chavchavadze avenue 2, 380028 Tbilisi, Republic of Georgia

⋆⋆ Research Associate of the Belgian National Fund for Scientific Research (NFWO).

niques recently it was revealed that inhomogeneous flows can host shear-induced, essentially linear phenomena with the *non-exponential, "nonmodal" temporal evolution*. In particular, it was found that:

- Waves sustained by the flow acquire the ability to exchange energy with the flow (Chagelishvili et al. 1994). These waves can damp or amplify at the cost of the free energy in the equilibrium flow. The similar phenomenon takes place in relativistic flows in a much more efficient way (Rogava et al. 1998b).
- In flows sustaining more than one type of wave motion, the shear provides a *linear* mechanism for their coupling and reciprocal transformations with corresponding energy exchange between the waves (Chagelishvili et al. 1996). The waves, of course, may still interact with the mean flow.
- Shear can lead to the excitation of characteristic beat waves both in hydrodynamic and hydromagnetic flows (Rogava & Mahajan 1997; Poedts et al. 1998; Rogava et al. 1999).
- Shear gives birth to a unique non-periodic mode of plasma collective behaviour: the algebraically (nonexponentially) evolving 'shear vortices' (Rogava et al. 1997; Rogava et al. 1998a). These vortices are able to extract energy from the mean flow either in the transient (2-D vortices) or in the asymptotic (3-D vortices) regimes. Hydrodynamic prototypes of these vortices are so called *Kelvin modes* (Lord Kelvin 1887; Marcus & Press 1977).
- In flows with moderate or high shearing rates, shear vortices eventually acquire wave-like features ("convert" into waves). This phenomenon occurs again in both the hydrodynamic (Chagelishvili et al. 1997c) and the plasma (Rogava et al. 1998a) channels.

Until recently all above itemized effects were considered for the simplest plane-parallel shear flows, with the plane Couette flow as an elementary archetype of the class. Yet, most astrophysical applications involve flows which are not plane-parallel. Recently, a new local method was developed (Mahajan & Rogava 1999) that allows to disclose and to study new classes of exotic collective modes in shear flows with *arbitrary* geometry and mean kinematics. [1] The method allows to consider velocity shear induced processes in those astrophysical situations, where deviation of the flow geometry and kinematics from the simple plane-parallel form are likely to be essential. It has become possible to investigate the whole set of astrophysical shear flows—from the most simplified to the most sophisticated.

This paper is dedicated to the one quite general and important class of astrophysical shear flows—cylindrically symmetric magnetohydrodynamic (MHD) flows. In particular, we consider a linear, axially magnetized flux tube with a spatially inhomogeneous axial plasma flow. This model is *concrete enough* for revealing of shear induced phenomena in all those astrophysical examples (e.g., accretion columns in X-ray pulsars, solar jet flows (spicules, surges, plumes), jets in protostars, Young Stellar Objects (YSO's), symbiotic stars and the Active Galactic Nuclei), where the mean geometry and kinematics of the flow patterns are roughly cylindrically symmetric. At the same time the model is *general enough* to be employed as a blueprint for more detailed and individualized quantitative models of each of these examples of astrophysical shear flows.

Applying the above mentioned *novel* method to this *new* setup we find that in cylindrical flows (like in plane-parallel flows) the MHD wave modes sustained by the system — the Alfvén (AW), the slow magnetosonic (SMW) and the fast magnetosonic (FMW) wave — become coupled through the agency of the velocity shear. The coupling is manifested in mutual transformations of these waves with corresponding energy exchange between them, complemented by the energy transfer between the waves and the background flow. This circumstance allows us to conclude that shear-induced wave transformations are characteristic not only for plane-parallel flow geometries, but are of a more universal nature.

Based on this issue we argue that the individual wave transformation events, happening perpetually and irregularly in the whole space occupied by the flow (Poedts et al. 1999), may establish the regime, where one should expect to observe an oscillating "blend" of different MHD waves throughout the flow, rather than this or that kind of wave activity. One can designate the ensuing state of (quasi)periodic energy transfer from one wave mode to the other and back as the state of *shear-driven wave oscillations*.

Essentially shear-driven wave oscillations may happen in a wide variety of plasma flows with different shearing rates and different values of $\beta \equiv 8\pi P_0/\mathcal{B}_0^2$, the ratio of the thermal to the magnetic energy. It is the plasma $\beta$, however, that determines which of the modes will effectively exchange energy. In particular for a high-$\beta$ plasma, the FMW do not participate in shear-driven wave oscillations, while the SMW and the AW do transform into one another. On the contrary, in the low-$\beta$ plasmas, SMW are unaffected, but FMW and the AW are involved in shear-driven oscillations. The situation is the most complicated in plasmas with $\beta$ close to unity, where all three wave modes are effectively coupled with each other and all kinds of transformations are likely to occur.

The flux tube MHD model that we explore in this paper is particularly apt in imitating some of the features of the "solar jet flows" (Shibata 1996). In addition, the solar atmosphere has just the right conditions for the development of all the above-mentioned wave oscillation regimes. Characteristic values of the plasma temperature $T$, the particle number density $N$, Alfvén $C_A$ and sound $C_S$ speed for different layers of the solar atmosphere (taken from Parker 1991) are given in Table 1. It shows that in the photosphere, the thermal pressure of the plasma greatly exceeds the magnetic pressure with a $\beta \simeq 10^4$. At this level the motions are mainly hydrodynamical excepting in the intense photospheric flux tubes where $\beta$ may be considerably smaller (but still greater than unity). In the chromospheric and coronal plasmas, the thermal pressure becomes smaller than the magnetic pressure, with a characteristic $\beta \simeq 10^{-2}$. Evidently

[1] A comparable method, valid for incompressible linear shear flows with uniform shearing rates, has been known in the hydrodynamic literature (Lagnado et al. 1984; Craik & Criminale 1986).

**Table 1.** Characteristic values of the temperature $T(K)$, number density $N(cm^{-3})$, Alfvén speed $C_a(cm/s)$, sound speed $C_s(cm/s)$, and thermal/magnetic energy ratio $\beta$ for solar plasmas.

| Regions | $T$ $(K)$ | $N$ $(cm^{-3})$ | $C_A$ $(cm/s)$ | $C_s$ $(cm/s)$ | $\beta$ |
|---|---|---|---|---|---|
| Phot. | $5.6\times10^3$ | $10^{17}$ | $6\times10^3$ | $0.9\times10^6$ | $2.3\times10^4$ |
| Chrom. | $7\times10^3$ | $2\times10^{10}$ | $1.2\times10^7$ | $1.1\times10^6$ | $10^{-2}$ |
| Cor. Hole | $1.5\times10^6$ | $10^8$ | $2\times10^8$ | $2\times10^7$ | $10^{-2}$ |

there must exist an intermediate region (at some variable height in the lower chromosphere) where $\beta\simeq1$. The reoccurrence of $\beta\simeq1$ plasma flows is, again, likely in the distant regions of the solar wind (Poedts et al. 1998).

In this article we solve a simple generic problem that covers a wide variety of astrophysical shear flows with cylindrical or roughly cylindrical geometry and kinematics; the solar magnetic plumes and spicules (macrospicules), for instance, will be systems where the present analysis could be gainfully applied. Observations of the chromospheric network and spicules indicate that vertical motions are well-pronounced and sufficient (in magnitude and in inhomogeneity) to play an important role in the energy balance (Athay 1986). Based on our studies of shear flows, we are inclined to argue that these vertical motions may play an important, even a dominant role in the processes of the MHD wave generation and regeneration, in the transmission of waves throughout the solar chromosphere and the transition region up to lower coronal heights, where the bulk of the coronal heating and major acceleration of the solar wind is believed to take place.

## 2. General formalism

We work within the framework of the standard magnetohydrodynamic equations:

$$D_t\rho + \rho\nabla\cdot\mathbf{V} = 0, \tag{1}$$

$$\rho D_t\mathbf{V} = -\nabla(P + B^2/8\pi) + (1/4\pi)(\mathbf{B}\cdot\nabla)\mathbf{B} + \rho\nu\Delta\mathbf{V}, \tag{2}$$

$$D_t\mathbf{B} = (\mathbf{B}\cdot\nabla)\mathbf{V} - \mathbf{B}\nabla\cdot\mathbf{V}, \tag{3}$$

$$\nabla\cdot\mathbf{B} = 0, \tag{4}$$

where $D_t\equiv\partial_t + \mathbf{V}\cdot\nabla$ is the convective (material) derivative and $\nu$ is the kinematic viscosity coefficient. The above set of equations needs to be complemented by "an equation of state" relating the thermal pressure to the density of the plasma. In this study we adopt an adiabatic MHD fluid approximation and employ $D_t(P\rho^{-\gamma}) = 0$ as a closure equation. This equation of state implies that the pressure and the density perturbations are linked through $p = C_S^2\rho$ where $C_S$ is the homogeneous speed of sound.

Let us consider a cylindrically symmetric flux tube with a stationary, axial plasma flow, and which is embedded in a vertically homogeneous ($\partial_z = 0$) and axisymmetric ($\partial_\phi = 0$) equilibrium magnetic field $\mathcal{B}_0$. By assumption, the field components are functions of $r$ alone, and may be expressed as (Sturrock 1994):

$$\mathbf{B}_0 = \{0,\ \mathcal{B}_\phi(r),\ \mathcal{B}_z(r)\}. \tag{5}$$

When the thermal pressure is radially homogeneous, the radial component of (2) imposes the following relation (with no viscosity) between the nonzero components of the equilibrium magnetic field:

$$r\mathcal{B}_z\partial_r\mathcal{B}_z + \mathcal{B}_\phi\partial_r(r\mathcal{B}_\phi) = 0. \tag{6}$$

This relation, coupled with the standard "uniform twist condition" of Gold and Hoyle (1958):

$$\mathcal{B}_\phi/\mathcal{B}_z = r(d\phi/dz)\equiv br,\ \ b = const, \tag{7}$$

yields

$$\mathcal{B}_\phi = b\mathcal{B}_0 r/(1 + b^2r^2), \tag{8a}$$

$$\mathcal{B}_z = \mathcal{B}_0/(1 + b^2r^2). \tag{8b}$$

When the twist parameter $b$ is zero, the field configuration reduces to the homogeneous, purely axial background field:

$$\mathbf{B}_0 = \{0,\ 0,\ \mathcal{B}_0\}. \tag{9}$$

The vertical force balance in the flux tube, governed by the $z$-component of the equation of motion, is similar to that of the pipe Poiseuille (Hagen-Poiseuille) flow in classic hydrodynamics

$$\partial_z\mathcal{P} = \rho\nu\partial_r^2\mathcal{U}_z, \tag{10a}$$

with the obvious solution:

$$\mathcal{U}_0(r)\equiv\mathcal{U}_r = U_m(1 - r^2/R^2), \tag{10b}$$

$$U_m\equiv(1/\rho\nu)\partial_z\mathcal{P}. \tag{10c}$$

Thus the *untwisted* flux tube comprises the Poiseuille-like flow of an MHD plasma in a uniform axial magnetic field (see Fig. 1). This model may serve as a zeroth order approximation for a wide variety of approximately cylindrical shear flows; it may also guide us in the construction of more realistic and sophisticated models like for the flux tube configurations in the context of the solar jet flow (Shibata 1996), or to study the physical processes in the galactic and extragalactic jets (Lovelace et al. 1991; Ferrari 1998).

In the appendix, we give a description of the method (Mahajan & Rogava 1999) for studying the nonexponentially evolving disturbances in shear flows with arbitrary velocity fields. In order to apply this method for the current model, we first note that in the close neighbourhood of an arbitrary point $A(x_0, y_0, z_0)$ ($|x - x_0|/|x_0|\ll1$, etc.), only two components of the *shear matrix* are nonzero

$$c_1 = -2U_m x_0/R^2, \tag{11a}$$

$$c_2 = -2U_m y_0/R^2, \tag{11b}$$

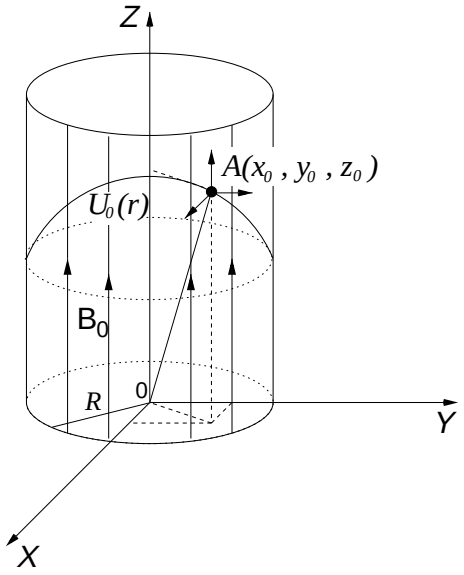


**Fig. 1.** Schematic sketch of a simple cylindrical flux tube with an axially parallel, stationary flow $\mathcal{U}_0(r)$ of the plasma and with a parallel and homogeneous equilibrium magnetic field $\mathcal{B}_0$.

that is, the background flow velocity may be approximated as

$$U_0(x,y)\simeq U_m + c_1 x + c_2 y. \tag{12}$$

Without loss of generality, we assume $c_1$ and $c_2$ to be positive.

With these approximations for the mean velocity, we are ready to write the set of linearized equations governing the local evolution of small-scale perturbations. These equations are the continuity equation

$$\mathcal{D}_t\rho + \rho_0(\partial_x v_x + \partial_y v_y + \partial_z v_z) = 0, \tag{13}$$

the three components of the equation of motion:

$$\mathcal{D}_t v_x = -(1/\rho_0)\partial_x P + (\mathcal{B}_0/4\pi\rho_0)[\partial_z B_x - \partial_x B_z], \tag{14a}$$

$$\mathcal{D}_t v_y = -(1/\rho_0)\partial_y P + (\mathcal{B}_0/4\pi\rho_0)[\partial_z B_y - \partial_y B_z], \tag{14b}$$

$$\mathcal{D}_t v_z + c_1 v_x + c_2 v_y = -(1/\rho_0)\partial_z P, \tag{14c}$$

and the transverse components of the induction equation

$$\mathcal{D}_t B_x = \mathcal{B}_0\partial_z u_x, \tag{15a}$$

$$\mathcal{D}_t B_y = \mathcal{B}_0\partial_z u_y, \tag{15b}$$

to be supplemented by:

$$\partial_x B_x + \partial_y B_y + \partial_z B_z = 0. \tag{16}$$

The initial value problem becomes solvable when one succeeds in finding a transformation annihilating the spatial dependence in the operator $\mathcal{D}_t \equiv \partial_t + U_0(x,y)\partial_z$. For our model, this is accomplished by the ansatz (A10) provided the wave vector $\mathbf{k}(t)$ acquires the time dependence given by the equations:

$$\partial_t k_x = -c_1 k_z, \tag{17a}$$

$$\partial_t k_y = -c_2 k_z, \tag{17b}$$

$$\partial_t k_z = 0, \tag{17c}$$

with the solution:

$$\mathbf{k}(t) = \{k_x(t) = k_x(0) - c_1 k_z t,\ k_y(t) = k_y(0) - c_2 k_z t,\ k_z\}; \tag{18}$$

the two variable components of the wave vector are linked by the relation $\Delta \equiv c_2 k_x(t) - c_1 k_y(t) = const$.

With this ansatz, the initial set (13-16) reduces to the following system of first-order ordinary differential equations (ODE's) for $\varrho(\mathbf{k},t)$, $\mathbf{u}(\mathbf{k},t)$, and $\mathbf{b}(\mathbf{k},t)$ which are, respectively, the spatial Fourier harmonics of $i\hat{\rho}(\mathbf{k},t)/\rho_0$, $\hat{\mathbf{v}}(\mathbf{k},t)$, and $i\hat{\mathbf{B}}(\mathbf{k},t)/\mathcal{B}_0$:

$$\partial_t \varrho = k_x(t)u_x + k_y(t)u_y + k_z u_z, \tag{19}$$

$$\partial_t u_x = -k_x(t)C_s^2\varrho + C_A^2[k_z b_x - k_x(t)b_z], \tag{20a}$$

$$\partial_t u_y = -k_y(t)C_s^2\varrho + C_A^2[k_z b_y - k_y(t)b_z], \tag{20b}$$

$$\partial_t u_z = -k_z C_s^2\varrho - c_1 u_x - c_2 u_y, \tag{20c}$$

$$\partial_t b_x = -k_z u_x, \tag{21a}$$

$$\partial_t b_y = -k_z u_y, \tag{21b}$$

complemented by the following algebraic relation between the magnetic field perturbation components:

$$k_x(t)b_x + k_y(t)b_y + k_z b_z = 0. \tag{22}$$

This is our *basic system*. In order to extract the underlying physical content, it is useful to show that the system (19-22) reduces to *a single* second order linear ordinary vector differential equation with variable coefficients:

$$\mathbf{F}^{(2)} + (\mathcal{W}^2 + \mathcal{C})\cdot\mathbf{F} = 0, \tag{23}$$

where the vector $\mathbf{F}$ is defined as

$$\mathbf{F} \equiv \{\Psi \equiv b_z - \varrho,\ b_x,\ b_y\}, \tag{24}$$

the diagonal "eigenfrequency matrix" $\mathcal{W}^2$ is:

$$\begin{pmatrix} C_s^2 k_z^2 & 0 & 0 \\ 0 & (C_A^2 + C_s^2)k_x^2(t) + C_A^2 k_z^2 & 0 \\ 0 & 0 & (C_A^2 + C_s^2)k_y^2(t) + C_A^2 k_z^2 \end{pmatrix}, \tag{25}$$

and the symmetric "coupling matrix" is defined as:

$$\mathcal{C} \equiv \begin{pmatrix} 0 & C_s^2 k_z k_x(t) & C_s^2 k_z k_y(t) \\ C_s^2 k_z k_x(t) & 0 & (C_A^2 + C_s^2)k_x(t)k_y(t) \\ C_s^2 k_z k_y(t) & (C_A^2 + C_s^2)k_x(t)k_y(t) & 0 \end{pmatrix}. \tag{26}$$

These equations can be derived by straightforward algebraic manipulations. In the component form, (23) reduces to the following set of coupled second-order ODE's:

$$\partial_t^2\Psi + C_s^2 k_z^2\Psi + C_s^2 k_z k_x(t) b_x + C_s^2 k_z k_y(t) b_y = 0, \tag{27a}$$

$$\partial_t^2 b_x + \left[(C_A^2+C_s^2)k_x^2(t)+C_A^2k_z^2\right]b_x + C_s^2k_zk_x(t)\Psi + (C_A^2+C_s^2)k_x(t)k_y(t)b_y = 0, \quad (27b)$$

$$\partial_t^2 b_y + \left[(C_A^2+C_s^2)k_y^2(t)+C_A^2k_z^2\right]b_y + C_s^2k_zk_y(t)\Psi + (C_A^2+C_s^2)k_x(t)k_y(t)b_x = 0. \quad (27c)$$

The physical meaning of the variable $\Psi$ becomes transparent when the induction Eq. (3) is written in the form:

$$D_t(\mathbf{B}/\rho) = (\mathbf{B}/\rho\cdot\nabla)\mathbf{V}, \quad (28)$$

suggested by Walen (1946); $\Psi$ is just the $z$-component of the perturbed "Walen" vector $\mathbf{B}/\rho$.

We also note that for the energy

$$E\equiv\frac{1}{2}\left[u_x^2+u_y^2+u_z^2+C_s^2\varrho^2+C_A^2(b_x^2+b_y^2+b_z^2)\right], \quad (29)$$

we can derive the evolution equation

$$\partial_t E = c_1[b_xb_z-u_xu_z]+c_2[b_yb_z-u_yu_z], \quad (30)$$

reminding us that $E$ is conserved in the "zero-shear" limit ($c_1 = c_2 = 0$).

One might form the erroneous impression that Eqs. (27) remain coupled even in the absence of shear. However, when $c_1 = c_2 = 0$ (zero shear limit) all coefficients in (27) become constants and one can decouple the equations and recover the fundamental (normal) frequencies of oscillation given by the following expected dispersion relation:

$$\left[\Omega^2-C_A^2k_z^2\right]\left[\Omega^4-(C_s^2+C_A^2)\mathbf{k}^2\Omega^2+C_s^2C_A^2k_z^2\mathbf{k}^2\right] = 0, \quad (31)$$

that has the well-known roots:

$$\Omega_A^2 = C_A^2k_z^2, \quad (32a)$$

$$\Omega_S^2 = \frac{1}{2}\left[(C_s^2+C_A^2)\mathbf{k}^2-\sqrt{(C_s^2+C_A^2)^2\mathbf{k}^4-4C_s^2C_A^2k_z^2\mathbf{k}^2}\right], \quad (32b)$$

$$\Omega_F^2 = \frac{1}{2}\left[(C_s^2+C_A^2)\mathbf{k}^2+\sqrt{(C_s^2+C_A^2)^2\mathbf{k}^4-4C_s^2C_A^2k_z^2\mathbf{k}^2}\right], \quad (32c)$$

corresponding to the AW, the SMW, and the FMW, respectively. The shear couples these modes in addition to imparting time dependence to the basic frequencies.

Yet another, less straightforward but more elegant way to expose the crucial role of the shear in the *physical* coupling of the MHD wave modes is to define the magnetic vorticity vector $\mathbf{\Omega}\equiv\mathbf{k}\times\mathbf{b}$ and to show that its longitudinal component, $\Omega_z$, obeys

$$\partial_t^2\Omega_z+\Omega_A^2\Omega_z = 2k_z^2(c_1u_y-c_2u_x), \quad (33)$$

while $\Psi$ obeys the following fourth order ODE:

$$\partial_t^4\Psi+(C_A^2+C_s^2)|\mathbf{k}|^2\partial_t^2\Psi+C_s^2C_A^2k_z^2|\mathbf{k}|^2\Psi = -2C_s^2k_z^3(c_1u_x+c_2u_y). \quad (34)$$

The last two equations clearly display the crucial role of the velocity shear in the physical coupling of the MHD modes. In the absence of shear ($c_1 = c_2 = 0$), Eq. (33) explicitly describes the AW, while (34) gives solutions for the SMW and the FMW without any coupling with one another and/or with AW.

## 3. Regimes of wave transformations

In order to probe further and quantitatively into the nature of the shear-induced wave transformations in various parameter regimes, we have to resort to numerical methods for solving the basic system of Eqs. (19-22). The following dimensionless notation: $\tau\equiv C_Ak_zt$, $\mathcal{K}_x(0)\equiv k_x(0)/k_z$, $\mathcal{K}_y(0)\equiv k_y(0)/k_z$, $\mathcal{K}_x(\tau)\equiv\mathcal{K}_x(0)-R_1\tau$, $\mathcal{K}_y(\tau)\equiv\mathcal{K}_y(0)-R_2\tau$, $v_i\equiv u_i/C_A$, $R_1\equiv(c_1/k_zC_A)$, $R_2\equiv(c_2/k_zC_A)$, and $\varepsilon\equiv C_s/C_A$, reduces the set (19-22) to:

$$\partial_\tau\varrho = \mathcal{K}_x(\tau)v_x+\mathcal{K}_y(\tau)v_y+v_z, \quad (35)$$

$$\partial_\tau v_x = -\mathcal{K}_x(\tau)\varepsilon^2\varrho+b_x-\mathcal{K}_x(\tau)b_z, \quad (36a)$$

$$\partial_\tau v_y = -\mathcal{K}_y(\tau)\varepsilon^2\varrho+b_y-\mathcal{K}_y(\tau)b_z, \quad (36b)$$

$$\partial_\tau v_z = -\varepsilon^2\varrho-R_1v_x-R_2v_y, \quad (36c)$$

$$\partial_\tau b_x = -v_x, \quad (37a)$$

$$\partial_\tau b_y = -v_y, \quad (37b)$$

$$\mathcal{K}_x(\tau)b_x+\mathcal{K}_y(\tau)b_y+b_z = 0. \quad (38)$$

For flows with weak shear, the coefficients in the preceding equations vary slowly, or adiabatically. This means that relative changes of these quantities during characteristic time scales of the problem are small. In this case the formulae (32) for normal frequencies are still useful for a qualitative description of the shear-induced dynamics (Chagelishvili et al. 1996; Poedts et al. 1998) of the wave modes. In dimensionless notation we have $\omega_a\equiv\Omega_A/C_Ak_z$, $\omega_s\equiv\Omega_S/C_Ak_z$, and $\omega_f\equiv\Omega_F/C_Ak_z$, and the expressions for the normal (fundamental) frequencies read [$\mathcal{K}^2(\tau)\equiv1+\mathcal{K}_x^2(\tau)+\mathcal{K}_y^2(\tau)$]:

$$\omega_a = 1, \quad (39a)$$

$$\omega_s(\tau) = \frac{\sqrt{2}}{2}\left[(1+\varepsilon^2)\mathcal{K}^2-\sqrt{(1+\varepsilon^2)^2\mathcal{K}^4-4\varepsilon^2\mathcal{K}^2}\right]^{1/2}, \quad (39b)$$

$$\omega_f(\tau) = \frac{\sqrt{2}}{2}\left[(1+\varepsilon^2)\mathcal{K}^2+\sqrt{(1+\varepsilon^2)^2\mathcal{K}^4-4\varepsilon^2\mathcal{K}^2}\right]^{1/2}. \quad (39c)$$

These are basically functions $\omega(\mathbf{k})$, which are given here as functions $\omega(\tau)$, as far as $\mathbf{k}(\tau)$ are explicit functions of time due to shear-induced temporal "drift" of $\mathbf{k}$. It is instructive to plot these "dispersion curves" as functions of time. The Alfvén dispersion curve is just a horizontal $\omega_a = 1$ line (Fig. 2) while the dispersion curve for the slow magnetosonic wave, $\omega_s(\tau)$ (the fast magnetosonic wave, $\omega_f(\tau)$) lies fully beneath (above) the $\omega_a = 1$ line, i.e., $\omega_s(\tau) < \omega_a < \omega_f(\tau)$.

Since the plasma $\beta$ is a determinant of the coupling efficiency between different modes, we present our numerical results in different $\beta$ regimes. We give a brief description of possible transformation regimes, illustrated by a number of corresponding plots.

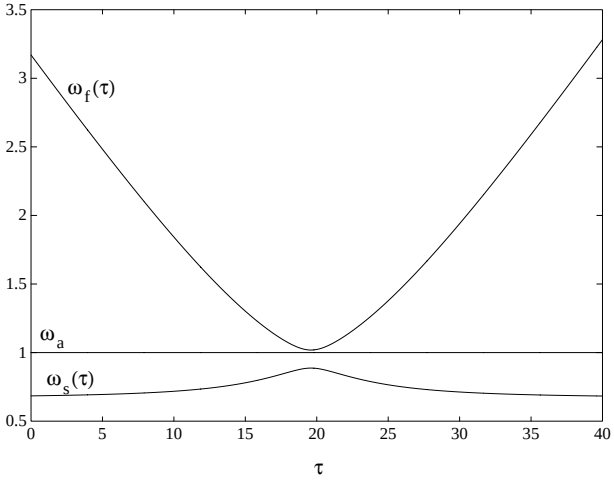


**Fig. 2.** Dispersion curves for the MHD waves, drawn for the case when $\varepsilon = 0.9$, $\mathcal{K}_x(0) = 0.9$, $\mathcal{K}_y(0) = 2$, $R_1 = 0.05$, and $R_2 = 0.1$. Note that the curves are the closest to one another when the function $\mathcal{K}_\perp^2(\tau) \equiv \mathcal{K}_x^2(\tau) + \mathcal{K}_y^2(\tau)$ acquires its minimum value.

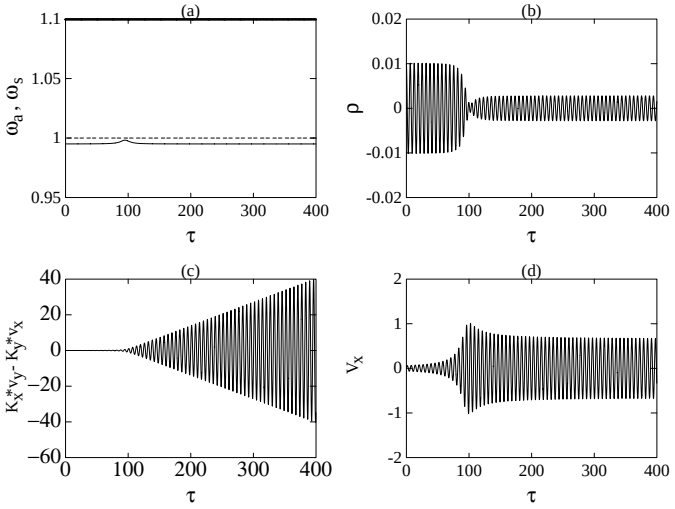


**Fig. 3a–d.** The transformation of the slow magnetosonic wave into the Alfvén wave in the high-$\beta$ plasma shear flow. The set of parameters is: $\varepsilon = 10$, $\mathcal{K}_x(0) = 10$, $\mathcal{K}_y(0) = 8$, $R_1 = 0.1$, and $R_2 = 0.09$. Fig. 3a shows dispersion curves for the coupled waves. Figs. 3b,c,d are drawn for the functions $\varrho$, $(\mathbf{k}\times\mathbf{v})_z$, and $v_x$, respectively.

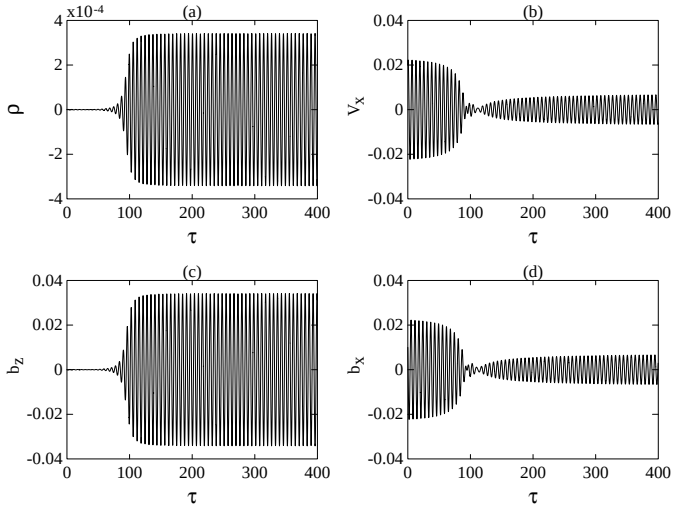


**Fig. 4a–d.** The transformation of the Alfvén wave into the slow magnetosonic wave. The same setup as on the Fig. 3, but for the case when the initial perturbation is a pure Alfvén wave. Figs. 4a,b,c,d are drawn for the functions $\varrho$, $v_x$, $b_z$, and $b_x$, respectively.

1. In **high-**$\beta$ plasmas with $\varepsilon^2 \gg 1$ it is easy to evaluate from (39b) and (39c) that the fast modes possess a time-dependent wave frequency $\omega_f(\tau) \simeq \varepsilon\mathcal{K}(\tau)$, while the frequency of the slow mode is almost constant with $\omega_s \simeq 1 = \omega_a$. In this situation, the dispersion curves for the slow and the Alfvén waves do come very close to each other whereas the dispersion curve of the fast wave passes well above the other dispersion curves. In the high-$\beta$ case, therefore, the fast waves are almost decoupled from the Alfvén and the slow waves, while the latter two are expected to transform effectively into one another.

   The evolution of an initially pure slow magnetosonic wave, for a high-$\beta$ system, is illustrated in Fig. 3. The following plasma parameters, and the wave numbers of the initial fluctuation are used for this example: $\varepsilon = 10$, $R_1 = 0.1$, $R_2 = 0.09$, $\mathcal{K}_x(0) = 10$ and $\mathcal{K}_y(0) = 8$. Since the initial perturbation is purely magnetosonic, the longitudinal ($z$) components of both $\mathbf{k}\times\mathbf{v}$ and $\mathbf{k}\times\mathbf{b}$ vectors will be initially zero. If the wave had to retain its initial identity through the evolution, both $\mathcal{K}_x v_y - \mathcal{K}_y v_x$ and $\mathcal{K}_x b_y - \mathcal{K}_y b_x$ would always remain zero. This is not what happens in reality, though. It is clear from Fig. 3, that close to the moment $\tau = 100$, the initial wave abruptly changes its character. First, we see that the amplitude of the density oscillations decreases, while the amplitude of the transverse velocity oscillations ($v_x$) becomes sharply larger. This is an indication that the perturbation has become less longitudinal and more transverse. Second, the perturbation acquires a rapidly increasing longitudinal component of $\mathbf{k}\times\mathbf{v}$. This proves that the initial slow magnetosonic wave gives birth to an Alfvén wave through the agency of the velocity shear induced wave coupling.

   The opposite process — when an Alfvén wave is converted into a slow magnetosonic wave — is also supported by the shear-coupling in this regime. An initially pure Alfvénic perturbation has $\varrho(0) = b_z(0) = v_z(0) = 0$, and $\mathbf{k}\cdot\mathbf{v} = 0$. We see in Fig. 4 (which is drawn for the same flow and perturbation parameters as Fig. 3, but now with a pure Alfvén wave at the beginning) that the wave changes its nature in the course of its evolution; substantial density and longitudinal magnetic field component perturbations are excited after $\tau = 100$. At the same time the amplitude of the transverse components ($v_x$ and $b_x$) noticeably decreases. The wave ceases to be purely transverse: $\mathbf{k}\cdot\mathbf{v}$ becomes nonzero. All these features confirm that the initial Alfvén wave is partially transformed into a slow magnetosonic wave.

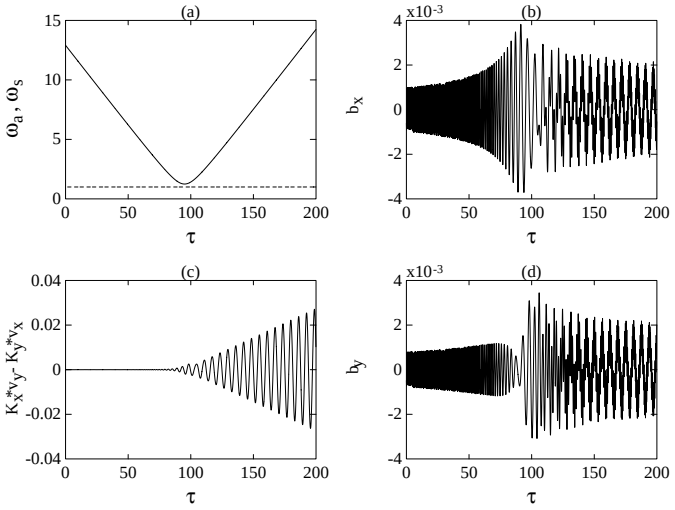


**Fig. 5a–d.** The transformations of the fast magnetosonic wave into the Alfvén wave in the low-$\beta$ plasma shear flow. The set of parameters is: $\varepsilon = 0.1$, $\mathcal{K}_x(0) = 10$, $\mathcal{K}_y(0) = 8$, $R_1 = 0.1$, and $R_2 = 0.09$. Fig. 5a shows dispersion curves for the coupled waves. Figs. 5b,c,d are drawn for the functions $b_x$, $(\mathbf{k}\times\mathbf{v})_z$, and $b_y$, respectively.

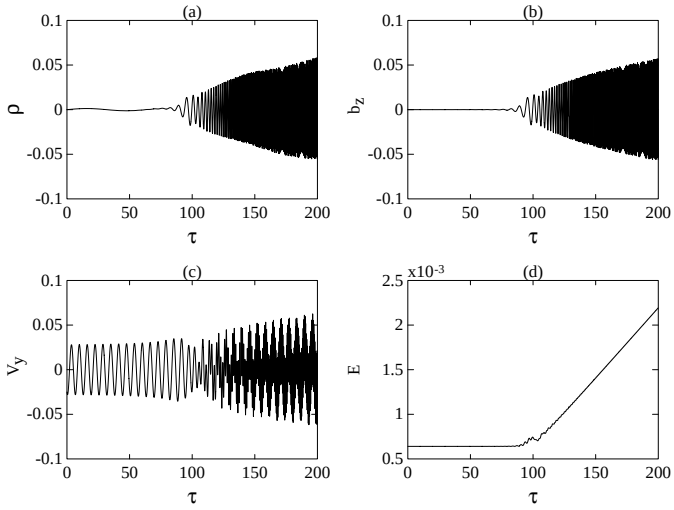


**Fig. 6a–d.** The transformation of the Alfvén wave into the fast magnetosonic wave. The same setup as on the Fig. 5, but for the case when the initial perturbation is a pure Alfvén wave. Figs. 6a,b,c,d are drawn for the functions $\varrho$, $b_z$, $v_y$, and $E$, respectively.

Thus we have shown that, in the flux tube shear flows of high-$\beta$ MHD plasmas, Alfvén waves and slow magnetosonic waves can readily transform into one another.

2. The **low-**$\beta$ plasmas with $\varepsilon \ll 1$ offer quite a different picture. In this case an estimate (Eq. (39b) and Eq. (39c)) of the frequencies $\omega_s \simeq \varepsilon/(1+\varepsilon^2)^{1/2}$, and $\omega_f \simeq \mathcal{K}(\tau) \equiv [1+\mathcal{K}_x^2(\tau)+\mathcal{K}_y^2(\tau)]^{1/2}$ suggests that the slow magnetosonic mode is decoupled from the other two MHD modes—its dispersion curve runs well below the Alfvén dispersion line and it is not expected to interact effectively with either mode. The fast magnetosonic wave, on the other hand, may effectively couple with the Alfvén mode for certain kinds of perturbations. For this to happen, the quantity $\mathcal{K}_\perp^2 \equiv \mathcal{K}_x^2(\tau)+\mathcal{K}_y^2(\tau)$ must have its minimum value close enough to zero so that the condition $\omega_f(\tau) \simeq \omega_s = 1$ is satisfied for a finite time interval.
   Some relevant examples of our numerical simulations are presented in Fig. 5 and Fig. 6. Apart from $\varepsilon = 0.1$, all other parameters are the same as in the previous cases. In Fig. 5, we display the time history of an initially pure fast magnetosonic wave. The emergence of clear low-frequency modulations in the transverse magnetic field components ($b_x$ and $b_y$), as well as the sharp appearance of the longitudinal component of the vorticity $\mathbf{k}\times\mathbf{v}$, definitely shows a partial conversion of the fast wave into the Alfvén wave.
   The opposite case, when the initial perturbation is purely Alfvénic, is illustrated in Fig. 6. Here, too, all features of an efficient wave transformation are present. Eventually, the perturbation acquires strong non-transversal features: high frequency oscillations in density as well as in the longitudinal magnetic field ($b_z$) appear. The $v_y$ component, which initially displays a constant frequency and constant amplitude Alfvén oscillations acquires, after the transformation, clear features of the high-frequency FSW which grows by extracting energy from the mean shear flow via the shear-induced processes. This process is a *bona-fide* signature of compressible (acoustic) waves in both hydrodynamic (Chagelishvili et al. 1994) and MHD (Rogava et al. 1996) shear flows. The time evolution of the total perturbation energy, as presented in Fig. 6, is quite representative.
   We conclude that the low-$\beta$ flux tube MHD shear flows support mutual transformations of the Alfvén and the fast magnetosonic waves.
3. The situation is rather complicated in plasmas with $\beta$ **close to unity**, where all three wave modes may be effectively coupled with one another. In this case it follows from (39b) and (39c) that $\omega_s(\tau) \simeq \mathcal{K}(1-\mathcal{K}_\perp/\mathcal{K})^{1/2}$ and $\omega_f(\tau) \simeq \mathcal{K}(1+\mathcal{K}_\perp/\mathcal{K})^{1/2}$. This means, again, that if the minimum value of $\mathcal{K}_\perp$ is close enough to zero then the regime $\omega_f(\tau) \simeq \omega_s(\tau) \simeq \omega_s = 1$ is realized and all three MHD wave modes may transform into each other.
   The threefold character of the transformations is illustrated in Figs. 7, 8, and 9. In Fig. 7 the evolution of the density perturbation indicates that the initial slow magnetosonic wave, with an almost constant frequency and amplitude, is converted into a complicated wave that has a distinct and increasing high-frequency component, the frequency corresponding to that of the fast wave. This is also clear from the time history plot of the total perturbation energy. Initially, the energy remains nearly constant, following adiabatically the dispersion curve of the slow wave, but after the transformation the energy begins to increase linearly following, at these times, the dispersion curve of the fast wave. However, the slow wave gives birth not only to the fast wave, but also to the Alfvén wave! This is evident from the plot of $\mathcal{K}_x v_y - \mathcal{K}_y v_x$ the presence of which is, as we already mentioned, a clear signature of the Alfvén mode.

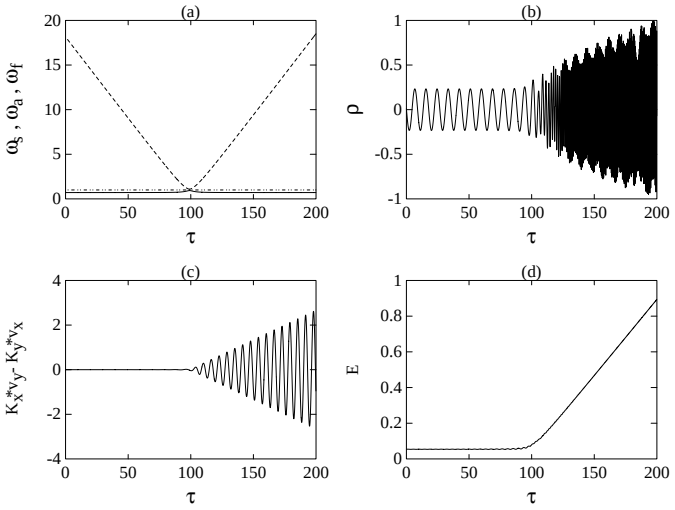


**Fig. 7a–d.** The transformation of the slow magnetosonic wave into the Alfvén wave and the fast magnetosonic wave in the $\varepsilon = 1$ case. The values of other parameters are: $\mathcal{K}_x(0) = 10$, $\mathcal{K}_y(0) = 8$, $R_1 = 0.1$, and $R_2 = 0.082$. Fig. 7a shows dispersion curves for the coupled waves. Figs. 7b,c,d are drawn for the functions $\varrho$, $(\mathbf{k}\times\mathbf{v})_z$, and $E$, respectively.

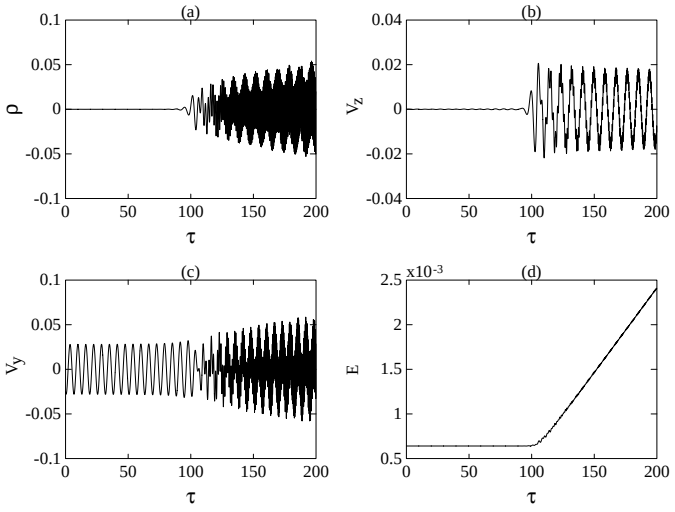


**Fig. 8a–d.** The transformation of the Alfvén wave into the fast magnetosonic wave and the slow magnetosonic wave in the $\varepsilon = 1$ case. Figs. 8a,b,c,d are drawn for the functions $\varrho$, $v_z$, $v_y$, and $E$, respectively.

In Fig. 8, our initial perturbation is a pure Alfvén wave. The important difference from the plot of Fig. 6 (showing the transformation of the Alfvén wave into the fast wave) is that, now, the transformed perturbation contains a slow wave component too. The density plot shows a clear low-frequency modulation of the dominant high-frequency fast magnetosonic wave.

Finally, Fig. 9 features the case, when the initial perturbation is the fast magnetosonic wave. The evolution of the total energy of the perturbation shows that the wave gives a substantial part of its energy to the mean flow and to the emerging low-frequency waves. One of these waves is evidently the Alfvén wave, because of the sharp appearance of the longitudinal component of the vorticity. The other wave is the almost constant frequency and constant amplitude slow magnetosonic wave featured in the plot for the longitudinal velocity component $v_z$.

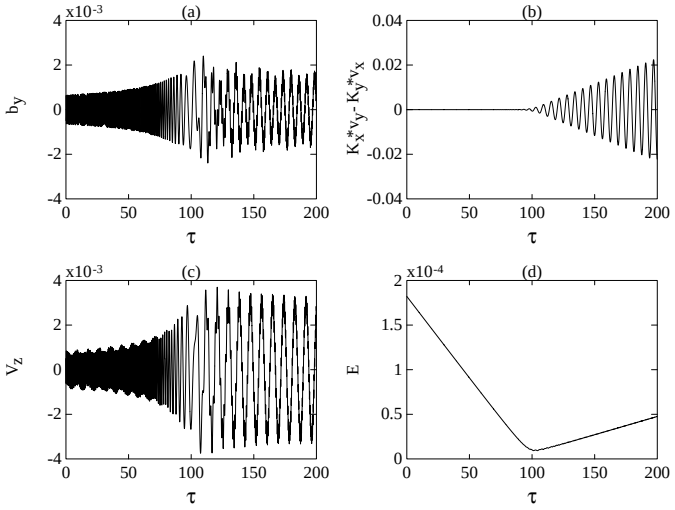


**Fig. 9a–d.** The transformation of the fast magnetosonic wave into the Alfvén wave and the slow magnetosonic wave in the $\varepsilon = 1$ case. Figs. 9a,b,c,d are drawn for the functions $b_y$, $(\mathbf{k}\times\mathbf{v})_z$, $v_z$, and $E$, respectively.

Another rather spectacular process, evoked in this regime by the shear-induced coupling of the MHD modes, is the appearance of the beat waves with the characteristic frequency equal to the half of the difference of the frequencies of two wave modes (Rogava & Mahajan 1997; Poedts et al. 1998) for the perturbations satisfying the condition $Max[R_1, R_2] \ll Max[\mathcal{K}_x(0), \mathcal{K}_y(0)] \ll 1$. This condition ensures a finite overlap of all three dispersion curves (see Fig. 10a) so that all three frequencies of normal oscillations are close to one another for a period long enough in comparison with the characteristic beat period. A clear appearance of the beat waves, as featured in Fig. 10, is then guaranteed.

## 4. Discussion

The results of the present study show that a cylindrical shear flow of a magnetized plasma provides favourable physical conditions for the onset of the velocity shear induced mutual transformations of MHD waves with corresponding energy exchange between the waves and between the waves and the background mean flow. This physical situation strongly resembles the one existing in plane-parallel shearing sheets of magnetized plasmas. In other words, we can argue that all kinds of *parallel shear flows*, irrespective of their spatial symmetry, exhibit shear induced wave transformations. The shear induced processes may play a crucial role in the understanding of two distinct kinds of physical phenomena:

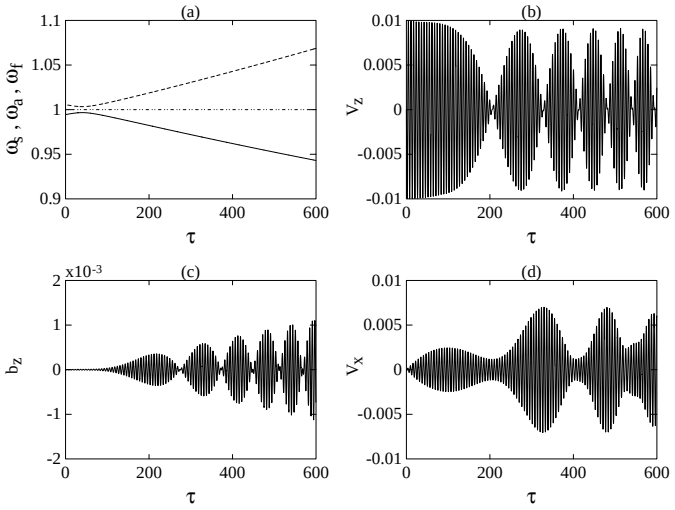


**Fig. 10a–d.** Beat waves [FMW-AW-SMW] displayed for the case when $\varepsilon = 1$, $\mathcal{K}_x(0) = 10^{-2}$, $\mathcal{K}_y(0) = 5{\times}10^{-3}$, $R_1 = 10^{-4}$, and $R_2 = 2{\times}10^{-4}$. The Fig. 10a shows the plot for the dispersion curves in this case, while Figs. 10b,c,d are drawn for the functions $v_z$, $b_z$, and $v_x$, respectively.

1. **Energy Exchange between waves and between the waves and the flow:** The principal message of the preceding calculations is that if a flow can sustain more than one wave mode and if there exists a mechanism to excite any of these, then under favorable conditions the shear induced processes can strongly couple these modes resulting in energy exchange between them. Individual modes, of course, may exchange energy with the flow. In the context of MHD flows (sustaining the Alfvén, the fast and the slow waves), we showed that physical parameters permitting, either of these three waves can generate any of the remaining two. In a shear flow, therefore, there exists the possibility of finding different kind of waves at different stages of the flow even though the external physical processes could generate only one of these. Beginning from any one of the MHD waves (AW, FMW, or SMW) the flow will convert them to a "mixture wave " consisting of the "primary" and the "secondary" (shear-generated) waves. In low $\beta$ plasmas, an initial input of an AW *or* a FMW will eventually evolve into a blend of both an AW *and* a FMW. In MHD plasmas with $\beta{\simeq}1$, initial waves of arbitrary kind (an AW, a FMW, or a SMW) will transform into the complex "wave soup" containing all three MHD modes. A similar situation pertains in high $\beta$ plasmas for a SMW and an AW.
2. **Nature of turbulence:** What does our study tell us about the nature of turbulence that may develop in hydromagnetic shear flows? The above analysis essentially implies that one should be quite careful when speaking about a particular kind of plasma turbulence (e.g., Alfvénic turbulence) in shear flows. Rather, in the background of a sheared flow, exhibiting a perpetually oscillating "sea" of mixed MHD waves, the turbulence that may develop is also likely to be of the "mixed" type.

After having described the shear-induced physical processes, we must look for possible examples of astrophysical flows in which we may see the manifestations of these physical phenomena. One important astrophysical situation, where shear induced wave oscillations may be very important is the solar atmosphere (Poedts et al. 1999). A short summary of the phenomenology follows.

It is widely known that the overall energy equilibrium of the solar atmosphere implies the dissipation of mechanical energy as heat and the subsequent expulsion of the heat input by radiation or by other processes like the accelerated solar wind. It is generally believed that the actual sources of the mechanical energy are the subphotospheric convection zone and rotation. But the exact sequence of physical processes that leads to the ultimate coronal heating and acceleration of the solar wind is still incompletely understood. In particular, it is known that even if the subphotospheric convection is able to generate all three kinds of MHD waves, only Alfvén waves are capable of making the whole trip through the chromosphere, penetrate through the transition region (the thermal boundary layer separating the solar chromosphere and corona) and reach the low coronal layers. But these waves, carrying an energy no more than $1{\times}10^5 ergs\ cm^{-2}s^{-1}$ are not energetic enough to account for the observed coronal heat input valued at $5-8{\times}10^5 ergs\ cm^{-2}s^{-1}$ level (Withbroe & Noyes 1977). Moreover, known theoretical mechanisms for Alfvén waves of $10^2 s$ period imply that they may dissipate effectively over distances $5-10R_s$, while analysis of the observed structure of the coronal hole by Withbroe (1988) shows that the major portion of the total coronal heat input is deposited in the first one or two solar radii.

The observed fine structure is a significant manifestation of the physical processes associated with energy and momentum exchange and balance in the solar atmosphere. The structure of the solar chromosphere is reasonably approximated as spherically symmetric for about the first 2000 km. Higher layers consist almost entirely of long, vertical columns rising above the general background and covering no more than $1\%$ of the solar surface. The individual vertical columns appear to be identical with *spicules* (Athay 1986) seen at the extreme limb, where the overall structure of the chromosphere resembles a "burning prairie." Together with low-lying relatively horizontal fibrils, spicules constitute the main elements of the chromospheric fine structure.

Observations provide knowledge about the morphological properties (lifetimes, dimensions, growth rates, geometry) of the chromospheric fine structure and also about its physical properties (thermodynamic conditions, streaming velocities, magnetic fields). This data suggests that spicules rise vertically, like slender magnetic flux tubes (filaments) out of the network beginning in the chromosphere and threading through the transition region into the low corona. Their average lifetime is 10-15 minutes, characteristic length scale $10.000km$, and characteristic diameter $700-1000km$ (Athay 1986). Flow velocities measured in spicules by Doppler shifts of spectral lines show mean velocities of $20-25km/s$. The estimated upward mass flux in

spicules is $10^{15}$ hydrogen atoms $cm^{-2}s^{-1}$. Since this is two orders of magnitude higher than the mass flux needed for the solar wind, it is usually admitted that the network downflow in the transition region is primarily the return flow of the spicule upheaval.

According to Athay (1986), therefore, the two most striking concepts emerging from fine structure studies are: (1) magnetic fields are widespread and play a crucial role in fine structure; and (2) fluid motions are of large amplitudes and clearly coupled with magnetic field structure. Going a step further we can admit that magnetic fields and fluid motions within spicules should somehow influence the propagation and morphology of MHD waves travelling throughout them. In this context we believe that the effect of shear-driven wave oscillations discussed in the present article is one of the highly probable physical processes that should be taken into account.

In particular, we argue that the fast magnetosonic waves that are amply produced by high-frequency photospheric motions within isolated intense magnetic flux tubes, become subject to shear-induced FMW-AW transformations in the chromosphere. The Alfvén waves, being weakly dissipative, and guided by spicules, are able to penetrate through the transition region and to reach those "heights" of the solar corona, where the main bulk of the coronal heating and the solar wind acceleration processes are generally believed to take place. The Alfvén waves contribute, by their pressure, to the acceleration of the solar wind. But the principal source of the acceleration may turn out to be the compressive damping of "secondary" fast waves—the outcome of the opposite (AW-FMW) transformation processes, evoked again by the velocity shear of the coronal flows! The principal advantage of this scenario is that it seems to *remove* the well-known problem with solar fast waves: the difficulty of their transmission throughout the highly reflective "shield"—transition region. Specifically, that part of FMW, which becomes converted into AW *below* the transition region passes through this region without substantial losses and later gives birth to "secondary" (internally generated) fast waves *above* the transition region.

In certain respect one may say that the shear-driven MHD wave oscillations bear a frail but attractive analogy with the oscillations of solar neutrinos.

Propagating MHD waves, network magnetic fields and direct plasma outflows are the likely physical factors that should contribute into the transmission of the mechanical energy to the chromosphere and corona. Since shear-driven oscillations of MHD waves is the phenomenon that genuinely implicates all these physical factors, it is quite reasonable to argue that this process should be elevated to an "important status" in the solar atmosphere.

*Acknowledgements.* S.M.M's work was supported in part by the U.S. Department of Energy Contract No. DE-FG03-96ER-54346. A.D.R's and S.P.'s work was supported in part by the INTAS grant No. 97-0504. A.D.R. wishes to thank Abdus Salam International Centre for Theoretical Physics and the 'Onderzoeksfonds K.U.Leuven' for supporting him, in part, through an Associate Membership Award (ICTP) and junior research fellowship (K.U.Leuven), respectively.

## Appendix A: nonexponentially evolving perturbations in arbitrary shear flows

Below we present a brief description of the method, suitable for studying the nonexponentially evolving disturbances in arbitrary shear flows (Mahajan & Rogava 1999).

Let us consider a background velocity field of the most general form:

$$\mathbf{U}(x,\,y,\,z)\equiv U_x(x,\;y,\;z)\mathbf{e}_x+U_y(x,\,y,\,z)\mathbf{e}_y+U_z(x,\,y,\,z)\mathbf{e}_z. \tag{A1}$$

In the close neighbourhood of a point $A(x_0,y_0,z_0)$, ($|x-x_0|/|x_0|\ll 1$, etc) we can expand all components $U_i(x,y,z)$ of the mean velocity field in Taylor series, preserving only linear terms of the expansion:

$$U_i(x,\;y,\;z)=U_i(A)\;+\;U_{i,x}(A)(x-x_0)+U_{i,y}(A)(y-y_0)\\ +\;U_{i,z}(A)(z-z_0). \tag{A2}$$

The nine constants $U_{i,k}(x_0,y_0,z_0)$ $(i,k=x,y,z)$ constitute the *Shear Matrix* $\mathcal{S}$:

$$\mathcal{S}\equiv\begin{pmatrix}U_{x,x} & U_{x,y} & U_{x,z}\\ U_{y,x} & U_{y,y} & U_{y,z}\\ U_{z,x} & U_{z,y} & U_{z,z}\end{pmatrix}\equiv\begin{pmatrix}a_1 & a_2 & a_3\\ b_1 & b_2 & b_3\\ c_1 & c_2 & c_3\end{pmatrix}. \tag{A3}$$

Note that for the flow with a *homogeneous* equilibrium density, the continuity equation demands

$$\nabla\cdot\mathbf{U}=0, \tag{A4}$$

which implies that the Shear Matrix, defined above, should be traceless:

$$a_1+b_2+c_3=0. \tag{A5}$$

Besides, one should also bear in mind that not all $\mathbf{U}(x,\;y,\;z)$'s are possible but only those which satisfy equilibrium state equations for the medium. Here we do not circumscribe the range of possible mean velocity fields, but give a scheme for a 'nonmodal' treatment of the perturbations for the most general case.

Adopting the convenient notation $U_{0i}=U_i(x_0,y_0,z_0)$ and $x_i\equiv x_i-x_{0i}$ we can write the following expressions for the components of (A1):

$$U_x(x,\;y,\;z)\simeq U_{0x}+a_1x+a_2y+a_3z, \tag{A6a}$$

$$U_y(x,\;y,\;z)\simeq U_{0y}+b_1x+b_2y+b_3z, \tag{A6b}$$

$$U_z(x,\;y,\;z)\simeq U_{0z}+c_1x+c_2y+c_3z. \tag{A6c}$$

For linear perturbations and for a velocity field $\mathbf{V}\equiv\mathbf{U}+\mathbf{u}$, the convective derivative of the velocity

$$[\partial_t+(\mathbf{V}\cdot\nabla)]\mathbf{V}=\partial_t\mathbf{u}+(\mathbf{U}\cdot\nabla)\mathbf{u}+(\mathbf{u}\cdot\nabla)\mathbf{U}, \tag{A7}$$

has the following components:

$$\mathcal{Q}u_x+a_1u_x+a_2u_y+a_3u_z, \tag{A8a}$$

$$\mathcal{Q}u_y + b_1u_x + b_2u_y + b_3u_z, \tag{A8b}$$

$$\mathcal{Q}u_z + c_1u_x + c_2u_y + c_3u_z, \tag{A8c}$$

where $\mathcal{Q}$ stands for the following linear operator:

$$\mathcal{Q}\equiv\partial_t+(U_{0x}+a_1x+a_2y+a_3z)\partial_x+(U_{0y}+b_1x+b_2y+b_3z)\partial_y + (U_{0z}+c_1x+c_2y+c_3z)\partial_z. \tag{A9}$$

Our chief concern is to eliminate spatial inhomogeneity, appearing in this convective derivative, by employing some specially selected ansatz for perturbations.

Let us try the representation:

$$F(x,\ y,\ z;\ t)\equiv\hat{F}(k_x(t),k_y(t),k_z(t);\ t)e^{i(\varphi_1-\varphi_2)}, \tag{A10a}$$

$$\varphi_1(x,y;t)\equiv k_x(t)x + k_y(t)y + k_z(t)z \tag{A10b}$$

$$\varphi_2(k_x(t),k_y(t),k_z(t);\ t)\ \equiv\ U_{0x}\int k_x(t)dt + U_{0y}\int k_y(t)dt + \ U_{0z}\int k_z(t)dt, \tag{A10c}$$

where, generally, $k_i(t)$ are components of the variable wave vector.

We must choose the time dependence of $k_i(t)$ so that the convective derivative becomes a simple time derivative. To go from

$$\begin{aligned}\mathcal{Q}F\ &=\ e^{i(\varphi_1-\varphi_2)}\partial_t\hat{F}\\ &+\ i\Big\{x\Big[k_x^{(1)}+a_1k_x+b_1k_y+c_1k_z\Big]\\ &+\ y\Big[k_y^{(1)}+a_2k_x+b_2k_y+c_2k_z\Big]\\ &+\ z\Big[k_z^{(1)}+a_3k_x+b_3k_y+c_3k_z\Big]\Big\}F.\end{aligned} \tag{A11}$$

to

$$\mathcal{Q}F = e^{i(\varphi_1-\varphi_2)}\partial_t\hat{F}, \tag{A12}$$

we require:

$$\partial_tk_x + a_1k_x + b_1k_y + c_1k_z = 0, \tag{A13a}$$

$$\partial_tk_y + a_2k_x + b_2k_y + c_2k_z = 0, \tag{A13b}$$

$$\partial_tk_z + a_3k_x + b_3k_y + c_3k_z = 0. \tag{A13c}$$

These equations may be written in the matrix notation:

$$\partial_t\mathbf{k} + \mathcal{S}^T\cdot\mathbf{k} = 0, \tag{36a}$$

with

$$\mathcal{S}^T\equiv\begin{pmatrix}a_1 & b_1 & c_1\\ a_2 & b_2 & c_2\\ a_3 & b_3 & c_3\end{pmatrix}, \tag{A15}$$

being the transposed shear matrix.

Note that up to now we did not make any assumptions on the details of the mean flow. Eqs. (A13), even in their the most general form, have simple analytic solutions, which embrace all possible kinds of background flows. Note also that Lagnado et al. (1984) and Craik & Criminale (1986) derived and used the same Eq. (A14) for $\mathbf{k}(t)$ for the case of incompressible linear flows with spatially uniform shearing rates.

## References


Athay R.G., 1986, In: Sturrock P.A. (ed.) Physics of the Sun. Vol. II, Reidel, Dordrecht, p. 51

Chagelishvili G.D., Rogava A.D., Segal I.N., 1994, Phys. Rev. E 50, 4283

Chagelishvili G.D., Rogava A.D., Tsiklauri D.G., 1996, Phys. Rev. E 53, 6028

Chagelishvili G.D., Khujadze G.R., Lominadze J.G., Rogava A.D., 1997a, Phys. Fluids 9, 1955

Chagelishvili G.D., Chanishvili R.G., Lominadze J.G., Tevzadze A.G., 1997b, Phys. Plasmas 4, 259

Chagelishvili G.D., Tevzadze A.G., Bodo G., Moiseev S.S., 1997c, Phys. Rev. Lett. 79, 3178

Craik A.D.D., Criminale W.O., 1986, Proc. R. Soc. London A 406, 13

Ferrari A., Trussoni E., Zaninetti L., 1981, MNRAS 196, 1051

Ferrari A., 1998, ARA&A 36, 539

Gold T., Hoyle F., 1958, MNRAS 120, 89

Joarder P.S., Nakariakov V.M., Roberts B., 1997, Solar Phys. 176, 285

Kelvin Lord (W. Thomson), 1887, Phil. Mag. 24, 188

Lagnado R.R., Phan-Thien N., Leal L.G., 1984, Phys. Fluids 27, 1094

Lovelace R.V.E., Berk H.L., Contopoulos J., 1991, ApJ 394, 459

Mahajan S.M., Rogava A.D., 1999, ApJ 518, 814

Marcus P., Press W.H., 1977, J. Fluid Mech. 79, 525

McKenzie J.F., 1970, Planet. Space Sci. 18, 1

Nakariakov V.M., Stepanyantz Y.A., 1994, Astron. Letters 20, 763

Nakariakov V.M., Roberts B., 1995, Solar Phys. 159, 213

Nakariakov V.M., Roberts B., Mann G., 1996, A&A 311, 311

Nakariakov V.M., Roberts B., Murawski K., 1998, A&A 332, 975

Parker E.N., 1964, ApJ 139, 690

Parker E.N., 1991, ApJ 372, 719

Poedts S., Rogava A.D., Mahajan S.M., 1998, ApJ 505, 369

Poedts S., Rogava A.D., Mahajan S.M., 1999, Space Sci. Rev. 87, 295

Rogava A.D., Mahajan S.M., Berezhiani V.I., 1996, Phys. Plasmas 3, 3545

Rogava A.D., Mahajan S.M., 1997, Phys. Rev. E 55, 1185

Rogava A.D., Chagelishvili G.D., Berezhiani V.I., 1997, Phys. Plasmas 4, 4201

Rogava A.D., Chagelishvili G.D., Mahajan S.M., 1998a, Phys. Rev. E 57, 7103

Rogava A.D., Berezhiani V.I., Mahajan S.M., 1998b, Phys. Scripta 58, 622

Rogava A.D., Poedts S., Heirman S., 1999, MNRAS 307, L31

Ryutova M.P., 1988, Sov. Phys. J.E.T.P. 94, 138

Ryutova M.P., Habbal S.R., 1995, A&A 451, 381

Shibata K., 1996, In: Tsinganos K.C. (ed.) Solar and Astrophysical Magnetohydrodynamic Flows. Kluwer, Dordrecht, p. 217

Singh A.P., Talwar S.P., 1994, Solar Phys. 149, 331

Sturrock P.A., 1994, Plasma Physics. Cambridge University Press, Cambridge

Walen C., 1946, Ark. Mat. Astr. Fys. 33A, 18

Withbroe G.L., 1988, ApJ 325, 442

Withbroe G.L., Noyes R.W., 1977, ARA&A 15, 363